Momentum stress jump condition at the fluid-porous boundary: Prediction of the jump coefficient.

Francisco J. Valdés-Parada[(a)], Benoît Goyeau[(b)] and J. Alberto Ochoa-Tapia[(a)*]

[(a)]División de Ciencias Básicas e Ingeniería; Universidad Autónoma Metropolitana-Iztapalapa; México, D.F., Mexico. E-mail: (Ochoa-Tapia) jaot@xanum.uam.mx; (Valdés-Parada) iqfv@xanum.uam.mx.

[(b)]FAST, UMR-CNRS 7608, Universités Paris VI et XI, Campus Universitaire, Bât 502, 91405 Orsay, Cedex, France. E-mail : goyeau@fast.u-psud.fr.

Introduction

Transport phenomena at the boundary between a porous medium and a fluid layer are the subject of intense research activity since they are involved in many industrial applications (catalytic reactors, dendritic solidifaction, drying processes, thermal insulation, etc.) or environmental situations (ground water pollution, benthic boundary layers, etc.). To study this kind of problems, two modeling approaches can be identified. In one hand, the one-domain approach considers the whole domain as a continuum where the transition between both fluid and porous regions is obtained through continuous spatial variations of properties[1,2,3,...]. On the other hand, in the two-domain approach the problem lies on coupling the conservation equations in both regions through the use of appropriate jump-boundary conditions at the fluid-porous inter-region[4,5,6,7,8,9]. However, these jump conditions often contain coefficients whose dependence on the local geometry of the interfacial region is missing. To include these effects, it is required to derive and solve the associated closure problems[10,11].

The problem of momentum transport (see Figure 1) was first studied by Beavers and Joseph[4], who proposed a semi-empirical slip boundary condition in order to couple the Stokes and Darcy equations. Later, using the method of volume averaging Ochoa-Tapia and Whitaker[7] (OT-W from here on) derived a jump boundary condition

$$\varepsilon_{\beta\omega}^{-1}\frac{\partial\left\langle v_\beta\right\rangle_\omega}{\partial y}-\frac{\partial\left\langle v_\beta\right\rangle_\eta}{\partial y}=\frac{\beta}{\sqrt{K_{\beta\omega}}}\left\langle v_\beta\right\rangle_\omega \quad \text{at } y=0 \tag{1}$$

to couple the Darcy-Brinkman and Stokes equations obtaining good agreement with the experimental results of Beavers and Joseph[12]. This condition was expressed in terms of an adjustable jump coefficient (β) which was determined to be of the order of the unity. Many attempts have been made to estimate the jump coefficient[13,14,15,16], however few of them have studied the physical meaning of this coefficient, furthermore an expression for β depending on the microstructure of the inter-region has yet to be obtained.

The objective of this work is to derive a stress jump boundary condition at the inter-region which does not involve adjustable coefficients. To this end, we closely follow the methodology described elsewhere (see ref. 11). Associated local closure problems, including the microstructure of the inter-region, are posed for the determination of a *mixed stress* tensor which is found to be the responsible of the jump. Since many of the steps involved in the derivation of the jump conditions are reported in Ochoa-Tapia and Whitaker[7], in the next section we will only show some of the main steps towards the derivation of the closed jump condition.

* **Corresponding author:** División de Ciencias Básicas e Ingeniería, Universidad Autónoma Metropolitana-Iztapalapa, Apartado Postal 55-534, México D.F., 09340, México. Email: jaot@xanum.uam.mx. Tel +(52) (55) 5724 4648; Fax: +52-55-58044900.

Methodology

The physical configuration considered here is the parallel fluid flow (η-region) over a homogeneous porous layer (ω-region) saturated by the same fluid[1] (see Figure 1). The flow is assumed to be stationary, incompressible and inertial effects in both regions are neglected. In Figure 1, the β-phase refers to the fluid phase while the solid phase refers to as the σ-phase. The local continuity and momentum conservation equations for the β-phase are the following

$$\nabla \cdot \mathbf{v}_\beta = 0, \qquad \text{in the } \beta-\text{phase} \tag{2}$$

$$0 = -\nabla p_\beta + \rho_\beta \mathbf{g} + \mu_\beta \nabla^2 \mathbf{v}_\beta, \qquad \text{in the } \beta-\text{phase} \tag{3}$$

with a no-slip boundary condition at the fluid-solid interface

$$\mathbf{v}_\beta = 0, \quad \text{at the } \beta-\sigma \text{ interface} \tag{4}$$

Averaging the above equations over a volume V yields after some manipulations (see Section 2 in ref. [7])

$$\nabla \cdot \langle \mathbf{v}_\beta \rangle = 0 \tag{5}$$

$$\begin{aligned} 0 = &-\nabla \langle p_\beta \rangle^\beta + \rho_\beta \mathbf{g} + \mu_\beta \varepsilon_\beta^{-1}(\mathbf{x}) \nabla^2 \langle \mathbf{v}_\beta \rangle \\ &-\mu_\beta \varepsilon_\beta^{-1}(\mathbf{x}) \nabla \varepsilon_\beta(\mathbf{x}) \cdot \nabla \left(\varepsilon_\beta^{-1}(\mathbf{x}) \langle \mathbf{v}_\beta \rangle \right) - \mu_\beta \mathbf{K}_\beta^{-1}(\mathbf{x}) \cdot \langle \mathbf{v}_\beta \rangle \end{aligned} \tag{6}$$

where $\varepsilon_\beta(\mathbf{x})$ is the fluid volume fraction (porosity) which depends on the location $\mathbf{x}$ of the centroid of the averaging volume. Since $\varepsilon_\beta(\mathbf{x}) = V_\beta(\mathbf{x})/V$, the volume fraction in both homogeneous regions reduces to

$$\varepsilon_\beta(\mathbf{x}) = \begin{cases} 1, & \text{in the } \eta-\text{region} \\ \varepsilon_{\beta\omega}, & \text{in the } \omega-\text{region} \end{cases} \tag{7}$$

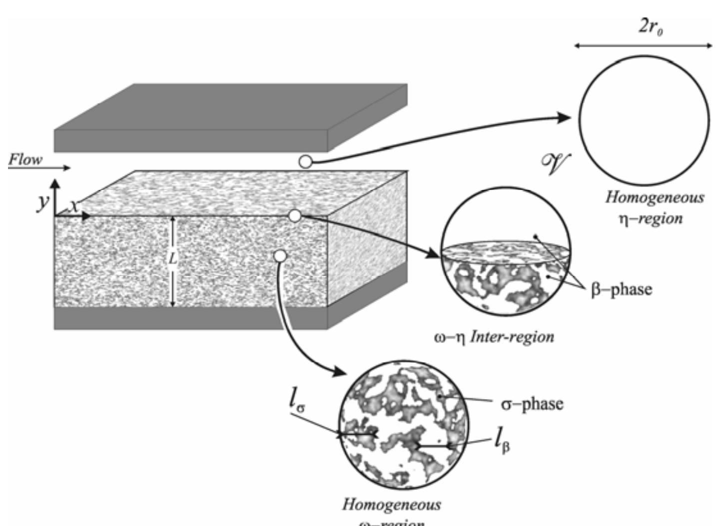

Figure 1: Averaging volume in both homogeneous regions and at the inter-region

In addition, in Eq. (6) we have introduced a position-dependent stress tensor, $\mathbf{K}_\beta^{-1}(\mathbf{x})$, defined by

$$\mu_\beta \mathbf{K}_\beta^{-1}(\mathbf{x})\cdot\langle \mathbf{v}_\beta\rangle = \frac{1}{V_\beta(\mathbf{x})}\int_{A_{\beta\sigma}(\mathbf{x})} \mathbf{n}_{\beta\sigma}\cdot\left(\mathbf{I}\tilde{p}_\beta - \mu_\beta \nabla\tilde{\mathbf{v}}_\beta\right)\mathrm{d}A$$
$$+\frac{1}{V_\beta(\mathbf{x})}\int_{A_{\beta\sigma}(\mathbf{x})} \mathbf{n}_{\beta\sigma}\cdot\left[\mathbf{I}\left(\left.\langle p_\beta\rangle^\beta\right|_{\mathbf{x}+\mathbf{y}_\beta} - \left.\langle p_\beta\rangle^\beta\right|_{\mathbf{x}}\right) + \mu_\beta\left(\left.\nabla\langle \mathbf{v}_\beta\rangle^\beta\right|_{\mathbf{x}} - \left.\nabla\langle \mathbf{v}_\beta\rangle^\beta\right|_{\mathbf{x}+\mathbf{y}_\beta}\right)\right]\mathrm{d}A \tag{8}$$

and, in the homogeneous regions, it becomes

$$\mathbf{K}_\beta^{-1}(\mathbf{x}) = \begin{cases} 0 & \text{in the } \eta-\text{region} \\ \mathbf{K}_{\beta\omega}^{-1} & \text{in the } \omega-\text{region} \end{cases} \tag{9}$$

In Eq. (8) $\tilde{p}_\beta$ and $\tilde{\mathbf{v}}_\beta$ are the pressure and velocity spatial deviations respectively, resulting from the spatial decompositions

$$p_\beta = \left.\langle p_\beta\rangle^\beta\right|_{\mathbf{x}+\mathbf{y}_\beta} + \tilde{p}_\beta \tag{10}$$

$$\mathbf{v}_\beta = \left.\langle \mathbf{v}_\beta\rangle^\beta\right|_{\mathbf{x}+\mathbf{y}_\beta} + \tilde{\mathbf{v}}_\beta \tag{11}$$

Since the derivation of Eqs. (5) and (6) does not involve the use of length-scale constraints, they are thus valid everywhere in the system[7].

In addition, when appropriate length scale constraints are satisfied ($l_\beta \ll r_0 \ll L$), Eqs. (5) and (6) reduce to the following

$$\nabla\cdot\langle \mathbf{v}_\beta\rangle_\eta = 0, \qquad \text{in the } \eta-\text{region} \tag{12}$$

$$0 = -\nabla\langle p_\beta\rangle_\eta^\beta + \rho_\beta \mathbf{g} + \mu_\beta \nabla^2\langle \mathbf{v}_\beta\rangle_\eta, \quad \text{in the } \eta-\text{region} \tag{13}$$

$$\nabla\cdot\langle \mathbf{v}_\beta\rangle_\omega = 0, \quad \text{in the } \omega-\text{region} \tag{14}$$

$$0 = -\nabla\langle p_\beta\rangle_\omega^\beta + \rho_\beta \mathbf{g} + \varepsilon_{\beta\omega}^{-1}\mu_\beta \nabla^2\langle \mathbf{v}_\beta\rangle_\omega - \mu_\beta \mathbf{K}_{\beta\omega}^{-1}\cdot\langle \mathbf{v}_\beta\rangle_\omega, \text{ in the } \omega-\text{region} \tag{15}$$

In order to complete the statement of the problem to determine the velocity profile, coupling boundary conditions at the inter-region are required. However, due to spatial variations of the micro-structure, the effective medium equations for the homogeneous regions are not valid at the inter-region. This difficulty can be overcome by the introduction of jump boundary conditions.

Following the work of OT-W leads to the condition of continuity of the normal component of the velocity

$$\mathbf{n}_{\omega\eta}\cdot\left(\langle \mathbf{v}_\beta\rangle_\omega - \langle \mathbf{v}_\beta\rangle_\eta\right) = 0 \qquad \text{at the } \omega-\eta \text{ inter-region} \tag{16}$$

while for the stress, the following jump boundary condition is obtained, following the recently reported methodology of Valdés-Parada et *al.*[11]

$$-\mathbf{n}_{\omega\eta}\left(\langle p_\beta\rangle_\omega^\beta - \langle p_\beta\rangle_\eta^\beta\right) + \mu_\beta \mathbf{n}_{\omega\eta}\cdot\left(\varepsilon_{\beta\omega}^{-1}\nabla\langle \mathbf{v}_\beta\rangle_\omega - \nabla\langle \mathbf{v}_\beta\rangle_\eta\right) = \frac{\mu_\beta}{a_{vs}}\mathbf{K}^{-1}\cdot\langle \mathbf{v}_\beta\rangle_\omega, \text{at the } \omega-\eta \text{ inter-region} \tag{17}$$

In Eq. (17) we have introduced a *mixed stress tensor*

$$\mathbf{K}^{-1} = \underbrace{\left.\mathbf{K}_\beta^{-1}\right|_{\eta\omega}}_{\text{global stress}} + \underbrace{\varepsilon_\beta^{-3}\left.\left(\nabla\varepsilon_\beta\cdot\nabla\varepsilon_\beta\right)\right|_{\eta\omega}\mathbf{I}}_{\text{Brinkman stress}} \tag{18}$$

which is actually a combination of the global and Brinkman stresses. Such combination was previously used by OT-W to define a drag vector **d**, whose tangent component is the adjustable parameter β. Let us note that both terms in $\mathbf{K}^{-1}$ are non-local quantities involving spatial variations of macroscopic properties. Comparing the tangential component of Eq. (17)

$$\frac{\partial \langle v_\beta \rangle_\omega}{\partial y} - \varepsilon_{\beta\omega} \frac{\partial \langle v_\beta \rangle_\eta}{\partial y} = \frac{K^{-1}}{a_{vs}} \varepsilon_{\beta\omega} \langle v_\beta \rangle_\omega, \text{at the inter-region } \eta - \omega \tag{19}$$

with the jump condition of OT-W (see Eq. (1)) gives

$$\beta = \frac{\sqrt{K_{\beta,\omega}} K^{-1}}{a_{vs}} \tag{20}$$

which indicates that the jump coefficient can be predicted by the determination of the tangential component (K^{1}) of $\mathbf{K}^{-1}$

$$K^{-1} = \mathbf{i} \cdot \mathbf{K}^{-1} \cdot \mathbf{i} = K_\beta^{-1}\Big|_{\eta\omega} + \varepsilon_\beta^{-3} \left(\frac{\mathrm{d}\varepsilon_\beta}{\mathrm{d}y} \right)^2 \Bigg|_{\eta\omega} \tag{21}$$

On the other hand, the Brinkman contribution can be evaluated by computing the spatial variations of the porosity. We found that such changes can be well approximated using the following polynomial

$$\varepsilon_\beta(y) = \frac{1}{2}(\varepsilon_{\beta\omega} + 1) + \frac{1}{4}(\varepsilon_{\beta\omega} - 1)\left(\frac{y}{r_0}\right)\left[\left(\frac{y}{r_0}\right)^2 - 3\right], \text{ for } -r_0 \le y \le +r_0 \tag{22}$$

so that the Brinkman stress is given by

$$\varepsilon_\beta^{-3} \left(\nabla \varepsilon_\beta \cdot \nabla \varepsilon_\beta \right)\Big|_{\eta\omega} = \frac{9}{2r_0^2} \frac{(\varepsilon_{\beta\omega} - 1)^2}{(\varepsilon_{\beta\omega} + 1)^3} \tag{23}$$

In addition, if the following length-scale constraints are met in the inter-region

$$\frac{l_\beta^2}{L_v L_{v1}} \ll 1; \quad \frac{r_0 l_\beta^2}{L L_v L_{v1}} \ll 1 \tag{24}$$

then, the global stress tensor (given in Eq. (8)) at the inter-region can be expressed in terms of the spatial deviations of pressure and velocity as

$$\mu_\beta \mathbf{K}_\beta^{-1}(\mathbf{x}) \cdot \langle \mathbf{v}_\beta \rangle\Big|_{\eta\omega} = -\frac{1}{V_\beta(\mathbf{x}_0)} \int_{A_{\beta\sigma}(\mathbf{x}_0)} \mathbf{n}_{\beta\sigma} \cdot \left(\mathbf{I}\tilde{p}_\beta - \mu_\beta \nabla \tilde{\mathbf{v}}_\beta \right) \mathrm{d}A, \text{ at the } \omega - \eta \text{ inter-region} \tag{25}$$

In this context, the dividing surface is located at the place where $\varepsilon_\beta = \frac{1}{2}(1 + \varepsilon_{\beta\omega})$ and is, from here on, designated as the position where the centroid is located at $\mathbf{x}_0$.

From Eq. (25), we have that, the determination of the permeability tensor at the inter-region can be achieved by solving the associated boundary value problems for the spatial deviations of pressure and velocity in a representative portion of the inter-region (see Figure 2). These problems are the result of subtracting Eqs. (5) and (6) to the local conservation equations (2) and (3)

$$\nabla \cdot \tilde{\mathbf{v}}_\beta = \underbrace{\varepsilon_\beta^{-1}(\mathbf{x}) \nabla \varepsilon_\beta(\mathbf{x}) \cdot \langle \mathbf{v}_\beta \rangle^\beta}_{\text{source}}, \qquad \text{in the } \beta-\text{phase} \tag{26}$$

$$\begin{aligned} 0 = & -\nabla \tilde{p}_\beta + \mu_\beta \nabla^2 \tilde{\mathbf{v}}_\beta - \underbrace{\mu_\beta \langle \mathbf{v}_\beta \rangle^\beta \varepsilon_\beta^{-1}(\mathbf{x}) \nabla^2 \varepsilon_\beta(\mathbf{x})}_{\text{source}} \\ & + \underbrace{\mu_\beta \varepsilon_\beta^{-1}(\mathbf{x}) \nabla \varepsilon_\beta(\mathbf{x}) \cdot \nabla \langle \mathbf{v}_\beta \rangle^\beta}_{\text{source}} + \underbrace{\mu_\beta \varepsilon_\beta(\mathbf{x}) \mathbf{K}_\beta^{-1}(\mathbf{x}) \cdot \langle \mathbf{v}_\beta \rangle^\beta}_{\text{source}}, \qquad \text{in the } \beta-\text{phase} \end{aligned} \tag{27}$$

Similarly, the boundary condition at the fluid-solid interface is obtained by introducing Eq. (11) in Eq. (4)

$$\tilde{\mathbf{v}}_\beta = \underbrace{-\left\langle \mathbf{v}_\beta \right\rangle^\beta}_{\text{source}}, \text{ at the } \beta-\sigma \text{ interface} \tag{28}$$

In order to complete the definition of the boundary-value problem for the spatial deviations, boundary conditions at the top and bottom of the unit cell shown in Figure 2, as well as periodicity conditions are imposed

$$\text{At } \zeta = -h \qquad \tilde{\mathbf{v}}_\beta = \tilde{\mathbf{v}}_\omega; \quad \tilde{p}_\beta = \tilde{p}_{\beta,\omega} \tag{29}$$

$$\text{At } \zeta = h \qquad \tilde{\mathbf{v}}_\beta = \tilde{\mathbf{v}}_\eta = 0; \quad \tilde{p}_\beta = \tilde{p}_{\beta,\eta} = 0 \tag{30}$$

$$\tilde{p}_\beta(\mathbf{r} + \ell_i) = \tilde{p}_\beta(\mathbf{r}), \; \tilde{\mathbf{v}}_\beta(\mathbf{r} + \ell_i) = \tilde{\mathbf{v}}_\beta(\mathbf{r}), \qquad i = 1,2 \tag{31}$$

Notice that, if the following length-scale constraints are satisfied at the inter-region

$$\frac{r_0}{L_v} \ll 1, \; \frac{r_0}{L_{v1}} \ll 1 \tag{32}$$

then both $\left\langle \mathbf{v}_\beta \right\rangle^\beta$ and its gradient can be taken as constants within the domain sketched in Figure 2. This allows the following expression for the deviation fields

$$\tilde{\mathbf{v}}_\beta = \mathbf{C}_\beta : \nabla \left\langle \mathbf{v}_\beta \right\rangle^\beta + \mathbf{B}_\beta \cdot \left\langle \mathbf{v}_\beta \right\rangle^\beta \tag{33}$$

$$\tilde{p}_\beta = \mu_\beta \mathbf{A}_\beta : \nabla \left\langle \mathbf{v}_\beta \right\rangle^\beta + \mu_\beta \mathbf{b}_\beta \cdot \left\langle \mathbf{v}_\beta \right\rangle^\beta \tag{34}$$

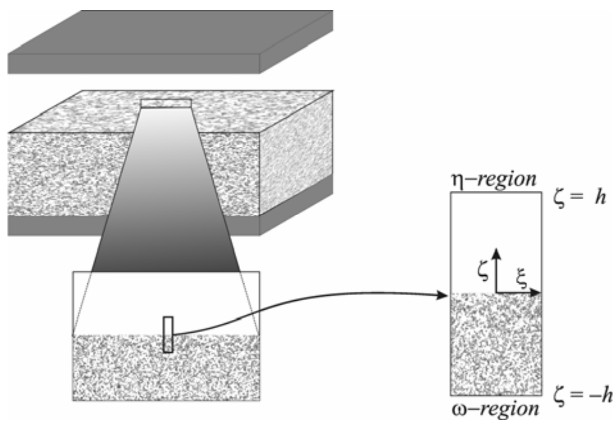

Figure 2: Representative zone of the inter-region.

Introducing the above equations in the boundary-value problem given by Eqs. (26)-(31), gives rise to two local closure problems. However, if the following constraint is satisfied

$$\frac{l_\beta^2}{r_0 L} \ll 1 \tag{35}$$

then only the closure variables $\mathbf{B}_\beta$ and $\mathbf{b}_\beta$ are needed to compute the spatial deviations fields and thus, the following boundary-value problem has to be solved

$$\nabla \cdot \mathbf{B}_\beta = \varepsilon_\beta^{-1}(\mathbf{x}_0) \nabla \varepsilon_\beta(\mathbf{x}_0), \qquad \text{in the } \beta-\text{phase} \tag{36}$$

$$\mathbf{0} = -\nabla \mathbf{b}_\beta + \nabla^2 \mathbf{B}_\beta - \varepsilon_\beta^{-1}(\mathbf{x}_0) \nabla^2 \varepsilon_\beta(\mathbf{x}_0) \mathbf{I} + \varepsilon_\beta(\mathbf{x}_0) \mathbf{K}_\beta^{-1}(\mathbf{x}_0), \quad \text{in the } \beta-\text{phase} \tag{37}$$

B.C.1 $\qquad \mathbf{B}_\beta = -\mathbf{I}, \qquad$ at the $\beta-\sigma$ interface $\qquad$ (38)

B.C.2 At $\zeta = h$ $\mathbf{B}_\beta = \mathbf{0};\ \mathbf{b}_\beta = \mathbf{0}$ (39)

B.C.3 At $\zeta = -h$ $\mathbf{B}_\beta = \mathbf{B}_\omega;\ \mathbf{b}_\beta = \mathbf{b}_\omega$ (40)

$$\text{Periodicity:}\quad \mathbf{b}_\beta(\mathbf{r}+\ell_i) = \mathbf{b}_\beta(\mathbf{r}),\ \mathbf{B}_\beta(\mathbf{r}+\ell_i) = \mathbf{B}_\beta(\mathbf{r}),\qquad i = 1,2 \tag{41}$$

In order to avoid, for the time being, the numerical difficulties of the "exact" solution of the closure problem, we propose to use a methodology to estimate the global contribution to the mixed permeability. This along with the evaluation of the Brinkman contributions at the inter-region, allows the estimation of the stress jump coefficient β.
The idea is to extrapolate the use of available expressions for the estimation of permeability in the bulk of the porous medium to the inter-region leading to,

$$K_\beta\big|_{\eta\omega} = \frac{\gamma \ell_\sigma^2 \left(1+\varepsilon_{\beta\omega}\right)^3}{2\left(1-\varepsilon_{\beta\omega}\right)^2} \tag{42}$$

where $\gamma = \gamma_1 = (180)^{-1}$, provides the well-known Carman-Kozeny equation while $\gamma = \gamma_2 = 2x10^{-3} / \left(1-\varepsilon_{\beta\omega}\right)^{2/3}$ leads to the results obtained by Larson-Higdon[17]. Using Eqs. (23) and (42) to estimate K^1 gives the following expression for β when substituted in Eq. (20)

$$\beta = \frac{2\varepsilon_{\beta\omega}^{3/2}}{3\sqrt{\gamma}\left(1+\varepsilon_{\beta\omega}\right)^3} \tag{43}$$

which depends only on the porosity and not on the characteristics of the microstructure. Actually, this later information is included in the associated closure problem, Eqs. (36)-(41), which needs to be solved in order to obtain an "exact" determination of the jump coefficient. Remember that $\beta \ll 1$ means that the effect of the heterogeneities at the inter-region are negligible.

In Figure 3 we show the effect of the porosity on β, note that the intersection of the curves corresponds to $\varepsilon_{\beta\omega}$ •0.79, which is the porosity of the Foametal samples used by Beavers and Joseph[4]. Furthermore, while the behavior of both models is the same as $\varepsilon_{\beta\omega} \to 0$ (even if this limit is not reachable for spheres), they provide different limits for $\varepsilon_{\beta\omega} \to 1$. However in the latter case, since the permeability of the porous medium tends to infinity, the R.H.S. of the tangential component of Eq. (17) tends to zero, which corresponds to the continuity of the velocity derivatives.

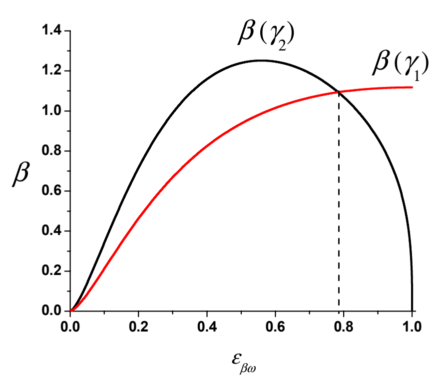

Figure 3: Dependence of the jump coefficient with the porosity using $\gamma = \gamma_1, \gamma_2$.

Moreover, the results for the jump coefficient (for Aloxite materials) using model χ_2 are found to be in good agreement with predictions previously reported in ref. [13]. Here we should insist that these observations are based on estimations and that only the solution of the closure problem can provide an accurate determination of the jump at the inter-region.

Conclusions

In this study, we have closely followed the methodology detailed in ref. [11], to derive a jump stress boundary condition free of adjustable jump coefficients. This jump condition involves a so-called *mixed stress tensor* which combines the Brinkman and global stress at the inter-region. The Brinkman contribution is evaluated from available expressions for the spatial variations of the porosity. Associated local closure problems, including the microstructure of the inter-region, have been derived for the determination of the global stress tensor. Due to the complexity of these problems, an approximate methodology has been proposed in order to quantify this contribution and estimate the tangential component of the mixed stress tensor. Furthermore, this component has been related to the stress jump coefficient in the boundary condition proposed by OT-W. The results for the jump coefficient (for Aloxite materials) are found to be in good agreement with predictions previously reported in ref. [13].

References

[1] E. Arquis, J.P. Caltagirone, Sur les conditions hydrodynamiques au voisinage d' un interface milieu fluide-milieu poreux : application à la convection naturalle. *C.R. Acad. Sci*. 1984; II 299: 1-4.

[2] C. Beckermann, R. Viskanta, S. Ramadhyani, Natural convection in vertical enclosures containing simultaneously fluid and porous layers. *Journal of Fluid Mechanics* 1988; 186: 257-284.

[3] D. Gobin, B. Goyeau, J.-P. Songbe, Double diffusive natural convection in a composite fluid-porous layer. *ASME Journal of Heat Transfer* 1998; 120: 234-242.

[4] G.S. Beavers, D.D. Joseph, Boundary conditions at a naturally permeable wall. *Journal of Fluid Mechanics* 1967; 30: 197-207.

[5] M. Prat, On the boundary conditions at the macroscopic level. *Transport in Porous Media* 1989; 4: 259-280.

[6] M. Sahraoui, M. Kaviany, Slip and no-slip temperature boundary conditions at the interface of porous plain media: Conduction. *International Journal of Heat and Mass Transfer* 1993; 36: 1019-1033.

[7] J.A. Ochoa-Tapia, S. Whitaker, Momentum transfer at the boundary between a porous medium and a homogeneous fluid-I: Theoretical development. *International Journal of Heat and Mass Transfer* 1995; 38(14): 2635-2646.

[8] J.A. Ochoa-Tapia, S. Whitaker, Heat transfer at the boundary between a porous medium and a homogeneous fluid. *International Journal of Heat and Mass Transfer* 1997; 40: 2691-2707.

[9] J.J. Valencia-López, G. Espinosa Paredes, J.A. Ochoa-Tapia, Mass transfer jump condition at the boundary between a porous medium and a homogeneous fluid. *Journal of Porous Media* 2003; 6: 33-49.

[10] B.D. Wood, M. Quintard, S. Whitaker, Jump condition at non-uniform boundaries: the catalytic surface. *Chemical Engineering Science* 2000; 55: 5231-5245.

[11] F.J. Valdés-Parada, B. Goyeau, J.A. Ochoa-Tapia, Diffusive mass transfer between a microporous medium and an homogeneous fluid: Jump boundary conditions. *Chemical Engineering Science* 2006; 61: 1692-1704.
[12] J.A. Ochoa-Tapia, S. Whitaker, Momentum transfer at the boundary between a porous medium and a homogeneous fluid- II: Comparison with experiment. *International Journal of Heat and Mass Transfer* 1995; 38(14): 2647-2655.
[13] B. Goyeau, D. Lhuillier, D. Gobin, M.G. Velarde, Momentum transport at a fluid-porous interface. *International Journal of Heat and Mass Transfer*. 2003; 46: 4071-4081.
[14] C. Deng, D.M. Martinez, Viscous flow in a channel partially filled with a porous medium and with wall suction. *Chemical Engineering Science* 2005; 60: 329-336.
[15] J.Y. Min, S.J. Kim, A novel methodology for thermal analysis of a composite system consisting of a porous medium and an adjacent fluid layer. *ASME Journal of Heat Transfer* 2005; 127: 648-656.
[16] M. Chandesris, D. Jamet, Boundary conditions at a planar fluid-porous interface for a Poiseuille flow. *International Journal of Heat and Mass transfer* 2006; 49 (13-14): 2137-2150.
[17] R.E. Larson, J.L. Higdon, A periodic grain consolidation model of porous media. *Physics of Fluids*. 1989; A1: 38-46.